

## Microporous Acidic Cesium Salt of 12-Tungstosilicic Acid $\text{Cs}_3\text{HSiW}_{12}\text{O}_{40}$ as a Size-selective Solid Acid Catalyst

Yuichi Kamiya,<sup>\*1</sup> Shogo Sano,<sup>2</sup> Yu-ki Miura,<sup>2</sup> Yohei Uchida,<sup>2</sup> Yuki Ogawa,<sup>2</sup> Yukari Iwase,<sup>2</sup> and Toshio Okuhara<sup>1</sup>

<sup>1</sup>Research Faculty of Environmental Earth Science, Hokkaido University, Sapporo, Hokkaido 060-0810

<sup>2</sup>Graduate School of Environmental Science, Hokkaido University, Sapporo, Hokkaido 060-0810

(Received May 17, 2010; CL-100472; E-mail: kamiya@ees.hokudai.ac.jp)

An acidic Cs salt of  $\text{H}_4\text{SiW}_{12}\text{O}_{40}$  ( $\text{Cs}_3\text{HSiW}_{12}\text{O}_{40}$ ), which was prepared by titrating an aqueous solution of  $\text{H}_4\text{SiW}_{12}\text{O}_{40}$  with an aqueous solution of  $\text{Cs}_2\text{CO}_3$ , possessed only micropores and exhibited size-selective catalysis for acid-catalyzed reactions in liquid phase.

Crystalline microporous oxides, such as zeolites, are useful materials for various applications, including catalysts, ion-exchange materials, adsorbents, and molecular sieves.<sup>1</sup> In catalysis, microporous oxides are able to act as size-selective catalysts due to their constrained pore size, and zeolites are typical examples of size-selective solid acid catalysts.<sup>2–4</sup> However, their applications are limited because the acid strengths are relatively weak. Thus, a variety of microporous oxides other than zeolites have been synthesized for potential use as solid acid catalysts.<sup>5–9</sup>

Heteropolyacids are oxide clusters with well-defined basic structures. They are fascinating and important catalysts from a practical standpoint because they are strong acids and are much more active than zeolites, such as H-ZSM-5, in various acid-catalyzed reactions.<sup>10–13</sup> Among heteropolyacids, the Keggin-type heteropolyacid  $\text{H}_3\text{PW}_{12}\text{O}_{40}$  and its acidic Cs salts have been extensively studied because of their high stability, strong acidity, and high surface area.<sup>10,11,14</sup> It has been reported that  $\text{Cs}_{2.1}\text{H}_{0.9}\text{PW}_{12}\text{O}_{40}$  (abbreviated as Cs2.1-*P*) is microporous<sup>15–17</sup> and that this acts as a size-selective catalyst for acid-catalyzed reactions.<sup>15</sup> In addition, its platinum-modified form shows size-selective catalytic activity toward the hydrogenation of alkenes and the complete oxidation of alkanes.<sup>18</sup>

In contrast, there are only a few reports involving Cs salts of  $\text{H}_4\text{SiW}_{12}\text{O}_{40}$ , though  $\text{H}_4\text{SiW}_{12}\text{O}_{40}$  is a Keggin-type heteropolyacid similar to  $\text{H}_3\text{PW}_{12}\text{O}_{40}$ . Moffat et al.<sup>19</sup> have reported that a neutral Cs salt of  $\text{H}_4\text{SiW}_{12}\text{O}_{40}$ ,  $\text{Cs}_4\text{SiW}_{12}\text{O}_{40}$ , is microporous with a high surface area ( $150\text{ m}^2\text{ g}^{-1}$ ), but the size of its micropores is uncertain. Blanco and co-workers have reported a synthesis of acidic Cs salts of  $\text{H}_4\text{SiW}_{12}\text{O}_{40}$ ,  $\text{Cs}_{3.4}\text{H}_{0.6}\text{SiW}_{12}\text{O}_{40}$  and  $\text{Cs}_{3.8}\text{H}_{0.2}\text{SiW}_{12}\text{O}_{40}$ , and their acid-catalytic activity toward phenol tetrahydropyranylation.<sup>20</sup> However, the salts that they prepared have mesopores as well as micropores, and thus, size-selective catalytic reactions over them have not been attempted. In this study, we synthesized microporous  $\text{Cs}_3\text{HSiW}_{12}\text{O}_{40}$  with little mesopores and a high surface area. Here we report that  $\text{Cs}_3\text{HSiW}_{12}\text{O}_{40}$  exhibits size-selective catalytic activity toward acid-catalyzed reactions in a liquid–solid reaction system. Since the formation mechanism of the micropores in  $\text{Cs}_3\text{HSiW}_{12}\text{O}_{40}$  is completely different from that in Cs2.1-*P* (discussed later), the pore sizes are different between the two, leading to different size-selective catalytic properties.

We prepared acidic Cs salts,  $\text{Cs}_3\text{HSiW}_{12}\text{O}_{40}$ , by titrating an aqueous solution of  $\text{H}_4\text{SiW}_{12}\text{O}_{40}$  ( $0.08\text{ mol dm}^{-3}$ ) with an aqueous solution of  $\text{Cs}_2\text{CO}_3$  ( $0.10\text{ mol dm}^{-3}$ ). In the preparation, the addition of aqueous  $\text{Cs}_2\text{CO}_3$  solution was carefully controlled by using an automatic syringe pump: first,  $2\text{ cm}^3$  was added at a rate of  $0.033\text{ cm}^3\text{ min}^{-1}$ , and then the remaining solution was added at a rate of  $0.2\text{ cm}^3\text{ min}^{-1}$ . The resulting colloidal solution was allowed to stand for 48 h at room temperature and then evaporated to obtain  $\text{Cs}_3\text{HSiW}_{12}\text{O}_{40}$  as a white solid. If one added the aqueous  $\text{Cs}_2\text{CO}_3$  solution to the aqueous solution of  $\text{H}_4\text{SiW}_{12}\text{O}_{40}$  at a constant rate of  $0.2\text{ cm}^3\text{ min}^{-1}$  from the beginning of the titration, fine particles with large external surface area were formed, which had adverse effects in the size-selective catalysis. Thus, the careful control of the addition of the aqueous  $\text{Cs}_2\text{CO}_3$  solution is very important.

Catalytic reactions (Figure S1<sup>21</sup>) were performed in a three-neck flask ( $100\text{ cm}^3$ ) after the catalysts were pretreated in a He flow at 473 K for 0.5 h. The reactions were carried out using isopropyl acetate (8 mmol) in *n*-decane (140 mmol) at 373 K, cyclohexyl acetate (14 mmol) in *n*-nonane (112 mmol) at 343 K, *tert*-butyl acetate (20 mmol) in *n*-decane (125 mmol) at 313 K,  $\alpha$ -pinene (0.64 mmol) in toluene (97 mmol) at 273 K, and cyclohexane (10 mmol) in 1,3,5-trimethylbenzene (216 mmol) at 363 K.

As shown in Figure 1, the changes in the surface area as a function of Cs content in  $\text{Cs}_x\text{H}_{4-x}\text{SiW}_{12}\text{O}_{40}$  were remarkable. The surface areas were estimated on the basis of a Langmuir plot obtained from an  $\text{N}_2$  adsorption isotherm at 77 K because all of

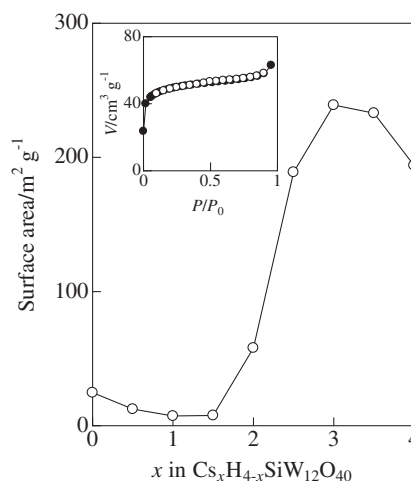


**Figure 1.** Surface area of  $\text{Cs}_x\text{H}_{4-x}\text{SiW}_{12}\text{O}_{40}$ . The surface area was determined from an  $\text{N}_2$  adsorption isotherm at 77 K after pretreatment of the catalyst at 473 K in a flow of  $\text{N}_2$ . Inset:  $\text{N}_2$  adsorption and desorption isotherm for  $\text{Cs}_3\text{HSiW}_{12}\text{O}_{40}$  at 77 K.

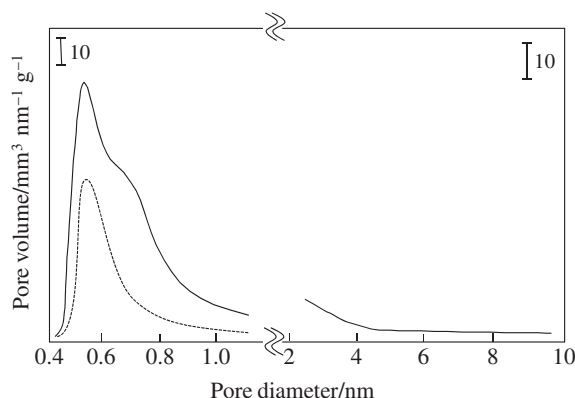


**Figure 2.** Micropore and mesopore size distributions for  $\text{Cs}_3\text{HSiW}_{12}\text{O}_{40}$  (solid line) and micropore size distribution for  $\text{Cs}_{2.1}\text{-P}$  (dotted line). Micropore size distribution was determined by using the Saito–Foley method on an Ar adsorption isotherm, and mesopore size distribution was determined by using the Dollimore–Heal method on an  $\text{N}_2$  desorption isotherm.

the Cs salts were microporous. The surface area increased significantly when the Cs content ( $x$ ) exceeded 1.5 and reached maximum at  $x = 3$  ( $239 \text{ m}^2 \text{ g}^{-1}$ ), although it decreased slightly when  $x > 3$ .

As shown in the inset of Figure 1,  $\text{Cs}_3\text{HSiW}_{12}\text{O}_{40}$  which had the highest surface area gave a types I isotherm of  $\text{N}_2$  adsorption–desorption at 77 K, indicating that this material was microporous. The total and external surface area were estimated from the slopes of two lines in a  $t$ -plot to be 191 and  $7 \text{ m}^2 \text{ g}^{-1}$ , respectively (Figure S2<sup>21</sup>). The external surface area corresponded to less than 4% of the total surface area.

In order to determine the micropore-size distribution of  $\text{Cs}_3\text{HSiW}_{12}\text{O}_{40}$ , we acquired an Ar adsorption isotherm at 87 K. Figure 2 shows pore-size distributions of the micropores as well as mesopores of  $\text{Cs}_3\text{HSiW}_{12}\text{O}_{40}$ . The micropore and mesopore size distributions were determined from the Ar adsorption isotherm by using the Saito–Foley method<sup>22</sup> and from an  $\text{N}_2$  adsorption isotherm by using the Dollimore–Heal method,<sup>23</sup> respectively. As a reference, micropore-size distribution of  $\text{Cs}_{2.1}\text{-P}$  is put in the figure. In the micropore-size distribution for  $\text{Cs}_3\text{HSiW}_{12}\text{O}_{40}$ , an intense peak at 0.53 nm and a shoulder at around 0.69 nm were observed. On the other hand, only a small amount of the mesopores was present.

The peak position for  $\text{Cs}_{2.1}\text{-P}$  was similar to that for  $\text{Cs}_3\text{HSiW}_{12}\text{O}_{40}$ , but the pore-size distribution was narrow and the larger-size micropores were nonexistent in it.

The size of the crystallites of  $\text{Cs}_3\text{HSiW}_{12}\text{O}_{40}$  was estimated to be about 49 nm from the line width in the X-ray diffraction (XRD) pattern. Assuming the external surface is only the surface of  $\text{Cs}_3\text{HSiW}_{12}\text{O}_{40}$ , the surface area was calculated from the density and the particle size to be  $19 \text{ m}^2 \text{ g}^{-1}$ . However, this value was significantly smaller than the actual surface area ( $239 \text{ m}^2 \text{ g}^{-1}$ ). This great difference can be explained if micropores are present inside the crystallites of  $\text{Cs}_3\text{HSiW}_{12}\text{O}_{40}$ .  $\text{Cs}_3\text{HSiW}_{12}\text{O}_{40}$  showed a XRD pattern due to body-centered cubic (bcc) structure (Figure S3<sup>21</sup>), in which the locations of heteropoly anion ( $\text{SiW}_{12}\text{O}_{40}^{4-}$ ) are allowable in the center and each corner of the unit cell, and that of  $\text{Cs}^+$  or  $\text{H}^+$  is between two heteropoly anions. To construct the bcc structure, heteropoly anion to cation

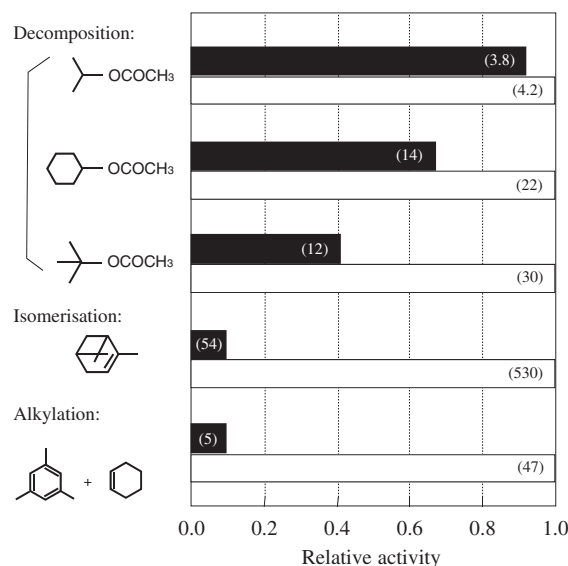


**Figure 3.** Relative activities of  $\text{Cs}_3\text{HSiW}_{12}\text{O}_{40}$  toward various kinds of reactions to those of  $\text{Cs}_{2.5}\text{H}_{0.5}\text{PW}_{12}\text{O}_{40}$  ( $\text{Cs}_{2.5}\text{-P}$ ) in the liquid–solid reaction system. The catalytic activity of  $\text{Cs}_{2.5}\text{-P}$  for each reaction is set to unity. The figures in the parentheses are the reaction rates in the unit of  $\text{mmol g}^{-1} \text{ h}^{-1}$ .

( $\text{Cs}^+$  and  $\text{H}^+$ ) ratio must be one third, while the actual ratio was one fourth due to the charge balance. Thus it would be expected that quarter heteropoly anions were defective, in other words, anion vacancies were present in the crystallites. Therefore, these anion vacancies formed the micropores of  $\text{Cs}_3\text{HSiW}_{12}\text{O}_{40}$ . In contrast to  $\text{Cs}_3\text{HSiW}_{12}\text{O}_{40}$ , the crystallites of  $\text{Cs}_{2.1}\text{-P}$  were nonporous.<sup>16</sup> Thus its micropores are considered to be inter-particle voids between the crystallites. The difference in the formation mechanism of the micropores results in micropore sizes between the two, though the size of heteropoly anions are very similar each other. Schlögl and co-workers have proposed a similar micropore structure for  $\text{Cs}_4\text{PMo}_{11}\text{VO}_{40}$  to  $\text{Cs}_3\text{HSiW}_{12}\text{O}_{40}$ .<sup>24</sup> However, at present, there is no direct evidence for the structure of the micropores in the crystallites of  $\text{Cs}_3\text{HSiW}_{12}\text{O}_{40}$ . Thus, further investigations are needed.

Figure 3 shows the relative catalytic activity of  $\text{Cs}_3\text{HSiW}_{12}\text{O}_{40}$  for each reaction in relation to those of  $\text{Cs}_{2.5}\text{H}_{0.5}\text{PW}_{12}\text{O}_{40}$  (abbreviated as  $\text{Cs}_{2.5}\text{-P}$ ).  $\text{Cs}_{2.5}\text{-P}$  has been shown to have micropores with sizes of more than 0.75 nm<sup>17</sup> and mesopores with sizes of ca. 4 nm<sup>16</sup> and does not exhibit any size-selective catalytic activity due to its large pore size.<sup>15</sup> As seen in Figure 3,  $\text{Cs}_{2.5}\text{-P}$  catalyzed all of the reactions with considerable activities (the reaction rates are shown in the parentheses in Figure 3). On the other hand, although  $\text{Cs}_3\text{HSiW}_{12}\text{O}_{40}$  was as active as  $\text{Cs}_{2.5}\text{-P}$  toward the decomposition of isopropyl acetate, the relative activity decreased in the following order: decomposition of isopropyl acetate > decomposition of cyclohexyl acetate > decomposition of *tert*-butyl acetate > isomerization of  $\alpha$ -pinene  $\approx$  alkylation of 1,3,5-trimethylbenzene.  $\text{Cs}_3\text{HSiW}_{12}\text{O}_{40}$  showed very low relative activity for the isomerization of  $\alpha$ -pinene and alkylation of 1,3,5-trimethylbenzene. After the reactions of the decomposition of isopropyl acetate,  $\text{Cs}_3\text{HSiW}_{12}\text{O}_{40}$  was recovered by a simple filtration from the mixture and dried at 373 K. The recovered  $\text{Cs}_3\text{HSiW}_{12}\text{O}_{40}$  showed similar

activity to the fresh one for the reactions. Critical sizes of the molecules were estimated from van der Waals radii and a molecular model obtained by using MM2 calculations to be the following: isopropyl acetate (0.52 nm) < cyclohexyl acetate (0.53 nm) < *tert*-butyl acetate (0.54 nm) <  $\alpha$ -pinene (0.61 nm) < 1,3,5-trimethylbenzene (0.77 nm). Although the critical size of *tert*-butyl acetate was similar to that of cyclohexyl acetate, the cross-sectional area of the former (0.54 nm  $\times$  0.46 nm) was much larger than that of the latter (0.53 nm  $\times$  0.37 nm). Therefore, the catalytic activity of Cs<sub>3</sub>HSiW<sub>12</sub>O<sub>40</sub> can be understood if the catalyst differentiates the reactant molecules according to their sizes; that is, it is size-selective.

In the case of the Cs<sub>x</sub>-P system, microporous Cs<sub>2</sub>.1-P showed reactant size selectivity in the acid-catalyzed reactions.<sup>15</sup> Cs<sub>2</sub>.1-P exhibited an activity for the dehydration of 2-hexanol but was inactive for the decomposition of isopropyl acetate due to the pore-size limitation.<sup>15</sup> On the other hand, as seen in Figure 3, Cs<sub>3</sub>HSiW<sub>12</sub>O<sub>40</sub> showed reasonably high activity for the decomposition of isopropyl acetate. This indicates that the pore size of Cs<sub>3</sub>HSiW<sub>12</sub>O<sub>40</sub> is larger than that of Cs<sub>2</sub>.1-P, which is consistent with the pore-size distributions shown in Figure 2. Therefore, Cs<sub>3</sub>HSiW<sub>12</sub>O<sub>40</sub> is a novel example of a heteropoly-acid catalyst showing size selectivity in reactions with larger sized reactants.

Typical 12-membered oxygen ring zeolites, such as H- $\beta$ , showed only one tenth of the activity of Cs<sub>3</sub>HSiW<sub>12</sub>O<sub>40</sub> for the decomposition of isopropyl acetate under the present reaction conditions. Since the pore size of H- $\beta$  (0.76 nm  $\times$  0.64 nm) is larger than the critical size of isopropyl acetate, the low activity was due to the weaker acid strength of the zeolites. Therefore, the strong acidity of Cs<sub>3</sub>HSiW<sub>12</sub>O<sub>40</sub> greatly contributes to the high activity toward the decomposition of isopropyl acetate and cyclohexyl acetate. We wish to emphasize that the much larger micropores and strong acidity of Cs<sub>3</sub>HSiW<sub>12</sub>O<sub>40</sub> expand the possible applications of microporous solid acids.

## References and Notes

- 1 D. W. Breck, *Zeolite Molecular Sieves: Structure, Chemistry, and Use*, Wiley, New York, **1974**.
- 2 *Shape-Selective Catalysis: Chemical Synthesis and Hydrocarbon Processing*, ed. by C. Song, J. M. Garcés, Y. Sugi, ACS Symposium Series 738, Washington, **1999**.
- 3 N. Y. Chen, W. E. Garwood, F. G. Dwyer, *Shape Selective Catalysis in Industrial Applications*, Marcel Dekker, New York, **1989**.
- 4 T. F. Degnan, Jr., *J. Catal.* **2003**, *216*, 32.
- 5 M. Sadakane, K. Kodato, T. Kuranishi, Y. Nodasaka, K. Sugawara, N. Sakaguchi, T. Nagai, Y. Matsui, W. Ueda, *Angew. Chem., Int. Ed.* **2008**, *47*, 2493.
- 6 X.-F. Shen, Y.-S. Ding, J. Liu, J. Cai, K. Laubernds, R. P. Zerger, A. Vasiliev, M. Aindow, S. L. Suib, *Adv. Mater.* **2005**, *17*, 805.
- 7 Q. Feng, H. Kanoh, K. Ooi, *J. Mater. Chem.* **1999**, *9*, 319.
- 8 K. Inumaru, H. Nakajima, T. Ito, M. Misono, *Chem. Lett.* **1996**, 559.
- 9 M. Fisch, T. Armbruster, B. Kolesov, *J. Solid State Chem.* **2008**, *181*, 423.
- 10 T. Okuhara, N. Mizuno, M. Misono, *Adv. Catal.* **1996**, *41*, 113.
- 11 I. V. Kozhevnikov, *Catal. Rev., Sci. Eng.* **1995**, *37*, 311.
- 12 C. L. Hill, C. M. Prosser-McCarthy, *Coord. Chem. Rev.* **1995**, *143*, 407.
- 13 N. Mizuno, M. Misono, *Curr. Opin. Solid State Mater. Sci.* **1997**, *2*, 84.
- 14 Y. Kamiya, T. Okuhara, M. Misono, A. Miyaji, K. Tsuji, T. Nakajo, *Catal. Surv. Asia* **2008**, *12*, 101.
- 15 T. Okuhara, T. Nishimura, M. Misono, *Chem. Lett.* **1995**, 155.
- 16 T. Yamada, Y. Yoshinaga, T. Okuhara, *Bull. Chem. Soc. Jpn.* **1998**, *71*, 2727.
- 17 T. Yamada, K. Johkan, T. Okuhara, *Microporous Mesoporous Mater.* **1998**, *26*, 109.
- 18 Y. Yoshinaga, K. Seki, T. Nakato, T. Okuhara, *Angew. Chem., Int. Ed. Engl.* **1997**, *36*, 2833.
- 19 D. B. Taylor, J. B. McMonagle, J. B. Moffat, *J. Colloid Interface Sci.* **1985**, *108*, 278.
- 20 L. R. Pizzio, M. N. Blanco, *Microporous Mesoporous Mater.* **2007**, *103*, 40.
- 21 Supporting Information is available electronically on the CSJ-Journal Web site, <http://www.csj.jp/journals/chem-lett/index.html>.
- 22 A. Saito, H. C. Foley, *Microporous Mater.* **1995**, *3*, 531.
- 23 D. Dollimore, C. R. Heal, *J. Colloid Interface Sci.* **1970**, *33*, 508.
- 24 S. Berndt, D. Herein, F. Zemlin, E. Beckmann, G. Weinberg, J. Schütze, G. Mestl, R. Schlögl, *Ber. Bunsen-Ges. Phys. Chem.* **1998**, *102*, 763.